

# In-Situ Measurements of $\Sigma$ ANs During INTEX-NA

Anne E. Perring<sup>1</sup>, Timothy H. Bertram<sup>1</sup>, Paul J. Wooldridge<sup>1</sup> and Ronald C. Cohen<sup>1,2</sup>

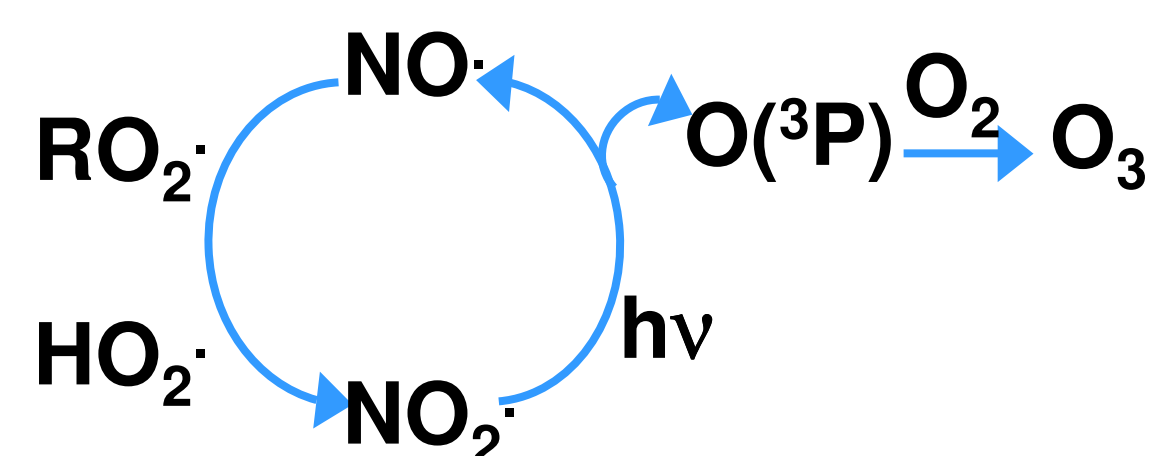
<sup>1</sup>Department of Chemistry; University of California, Berkeley, CA, 94720

<sup>2</sup>Department of Earth and Planetary Science; University of California, Berkeley, CA 94720

## Abstract

Alkyl and multifunctional nitrates ( $\Sigma$ ANs), produced by reactions of peroxy radicals with NO and reactions of the  $\text{NO}_3$  radical with alkenes, have previously been observed at high mixing ratios and comprising large fractions of  $\text{NO}_y$  and  $\text{NO}_z$  at the surface (Day et. al, 2003).  $\Sigma$ ANs were measured in real time aboard the NASA DC8 during INTEX-NA (6/1/04-8/14/04) by Thermal Dissociation Laser Induced Fluorescence (TD-LIF). Here we describe the first observations of  $\Sigma$ ANs above the surface. Aircraft flights during INTEX-NA included extensive characterization of the continental and marine boundary layers as well as frequent vertical profiles. Correlations between  $\Sigma$ ANs and other hydrocarbon oxidation products, such as formaldehyde and ozone, were used to constrain isoprene nitrate yields and to examine factors governing ozone production efficiency in the troposphere.

## The $\text{NO}_x$ Cycle



Radical-chain termination reactions:

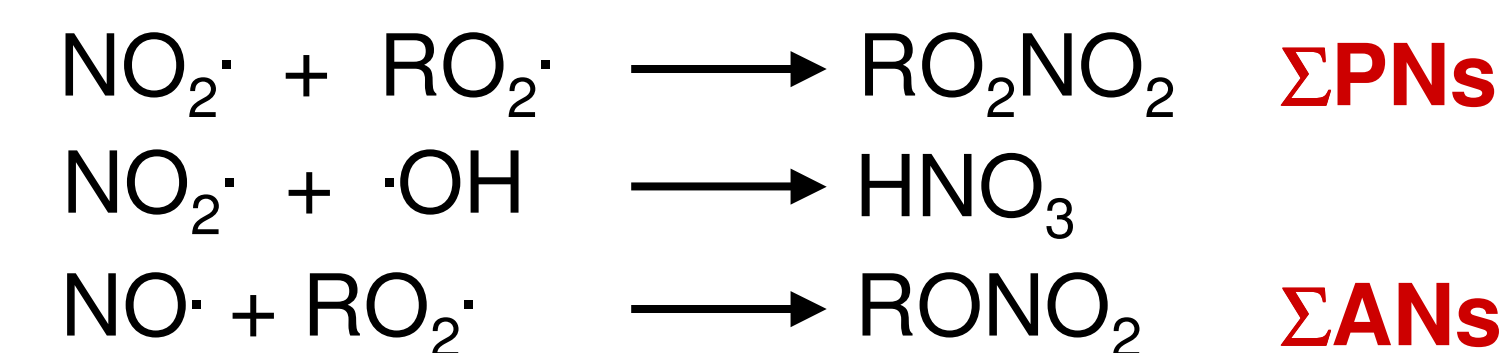
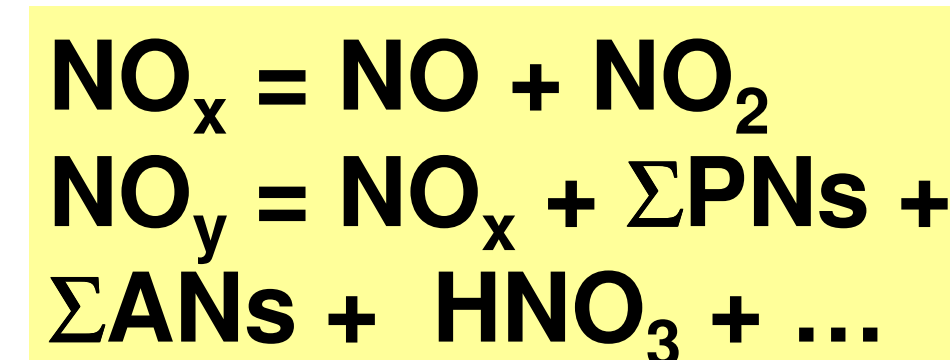


Figure 1: Tropospheric ozone is produced through coupled  $\text{HO}_x$  and  $\text{NO}_x$  cycles in a radical chain of events that continues unless one of the chain-termination reactions occur.



## $\Sigma$ ANs in the troposphere

Observations of  $\Sigma$ ANs made during INTEX-NA show that  $\Sigma$ ANs comprise a significant portion of  $\text{NO}_y$  throughout the lower troposphere. The observed concentrations of  $\Sigma$ ANs indicate that they could be a  $\text{NO}_x$  sink of comparable importance to  $\text{HNO}_3$ . Figure 2 shows the  $\text{NO}_y$  distribution for a single low-altitude segment of flight 10 that occurred in the boundary layer over a forested area. Figure 3 shows  $\text{NO}_y$  partitioning as a function of altitude averaged over flight 7.

## $\text{NO}_y$ in the boundary layer

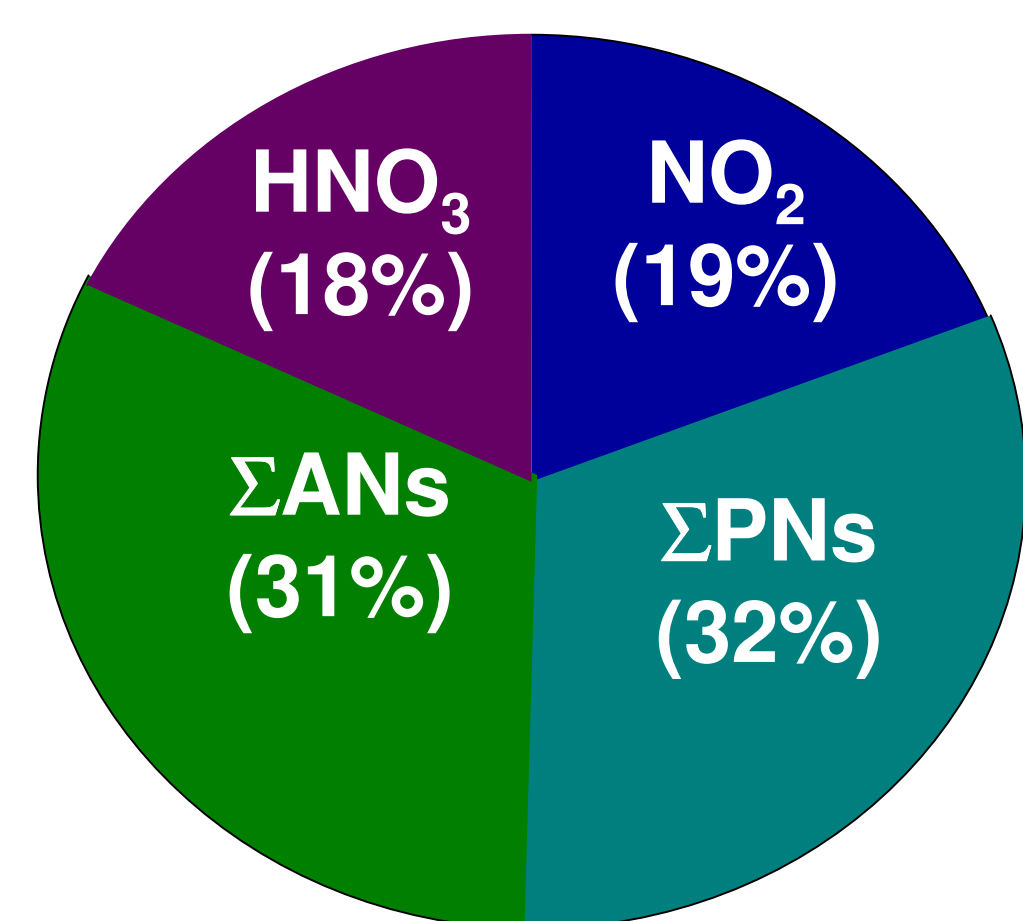


Figure 2: Low Altitude (<300 meters) Distribution of  $\text{NO}_y$  Measured by TD-LIF during the third low-level flight leg on 7/20/2004 while flying over a forested area.  $\text{HNO}_3$  data provided by Wennberg et al., CalTech

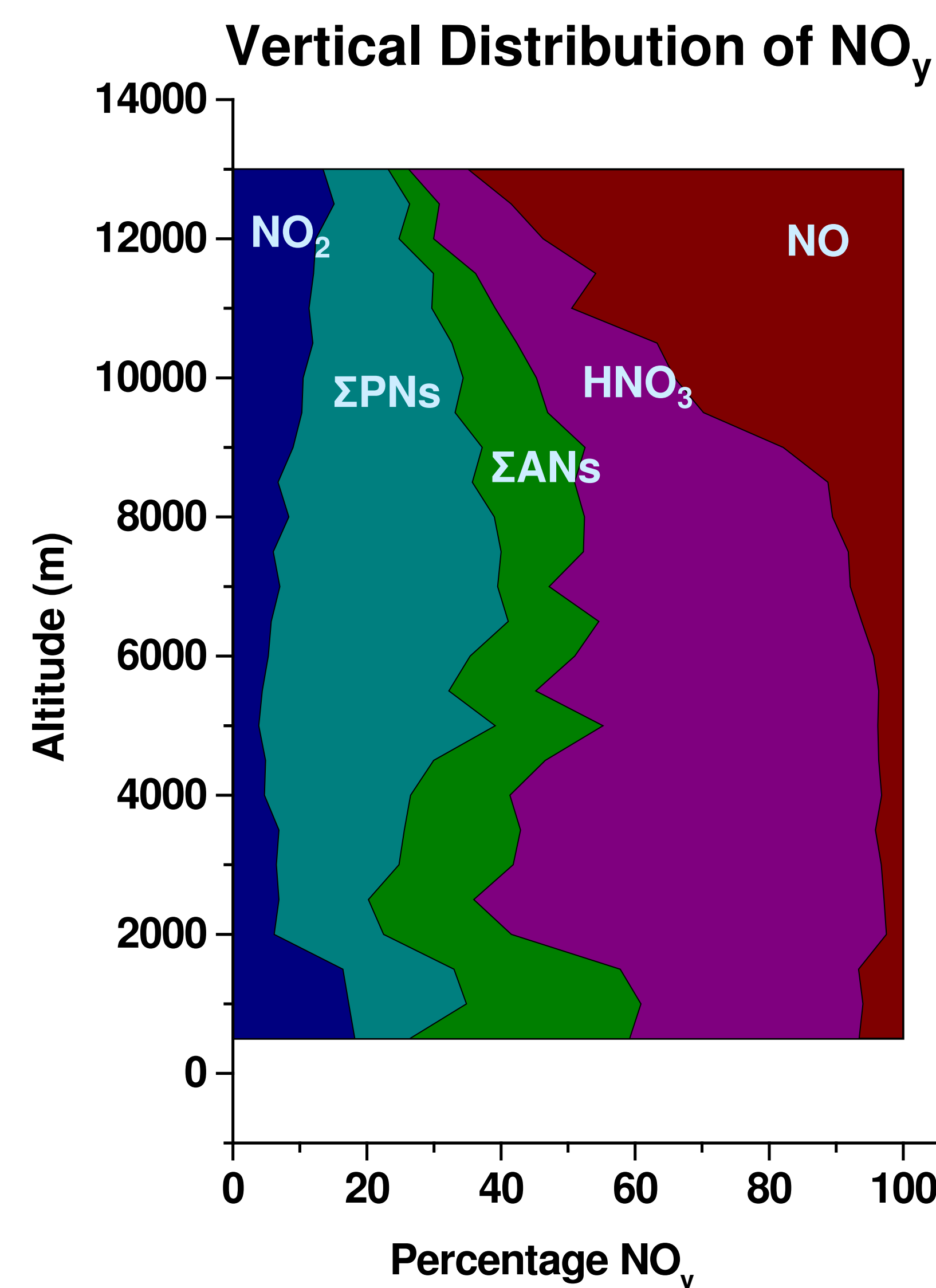
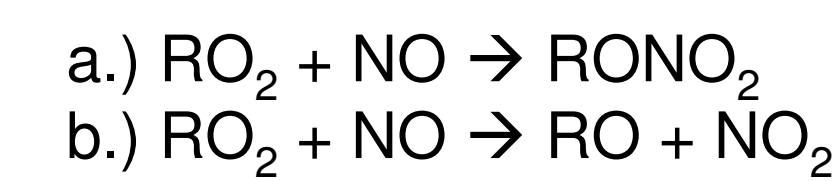


Figure 3: Profile of  $\text{NO}_y$  distribution on 7/12/2004 as a function of altitude.  $\text{NO}_2$ ,  $\Sigma\text{PNs}$  and  $\Sigma\text{ANs}$  measured by TD-LIF,  $\text{HNO}_3$  by chemical ionization mass spectrometry (Wennberg et al., CalTech) and  $\text{NO}$  calculated using steady state approximation.

## The formation of ANs and the importance of isoprene nitrates

Alkyl nitrates are formed as a minor product of the reaction between peroxy radicals and NO:



The ratio  $K_a/(K_a+K_b)$  is defined as the branching ratio and this sets the relative importance of chain termination and propagation. The branching ratio is dependent on the identity of R, increasing with size of the R group. The structural dependence of the branching ratio is well known for straight-chain alkanes and 1-alkenes but has been much harder to measure for certain other atmospherically relevant species such as isoprene. (Fig. 4)

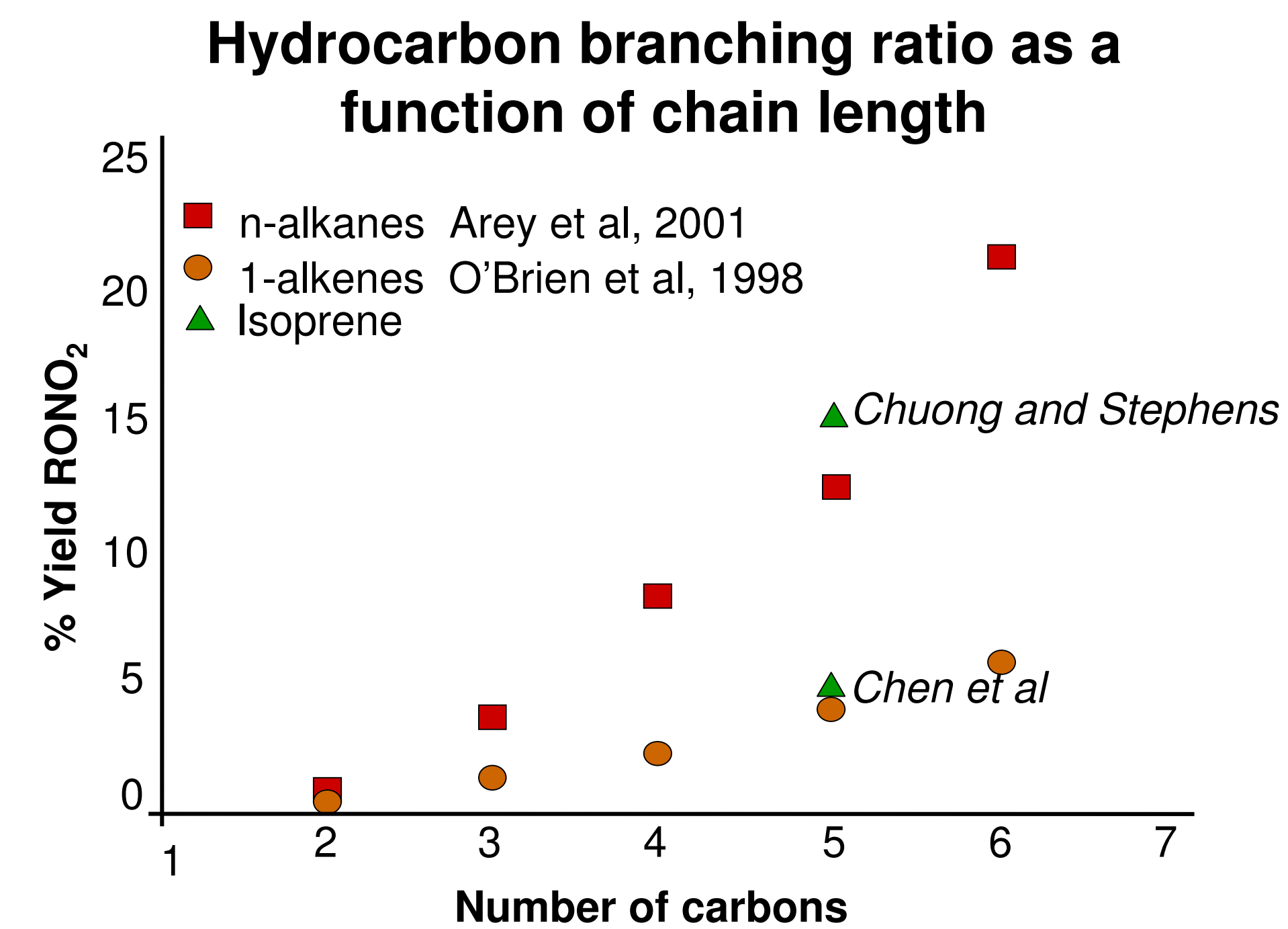


Figure 4: Carbon chain length v. published values of percent yield  $\text{RONO}_2$  (branching ratio). Published values for isoprene vary from 4.4 - 15%.

Isoprene is a 5-carbon dialkene which plays a large role in the production of tropospheric ozone. Yearly emissions are estimated at 500 Tg/yr making it the most important biogenic non-methane hydrocarbon in the atmosphere. (Guenther et al. 1995). The relative importance of isoprene in the ozone production cycle as compared to other hydrocarbons can be assessed using an OH reactivity-weighted hydrocarbon budget.

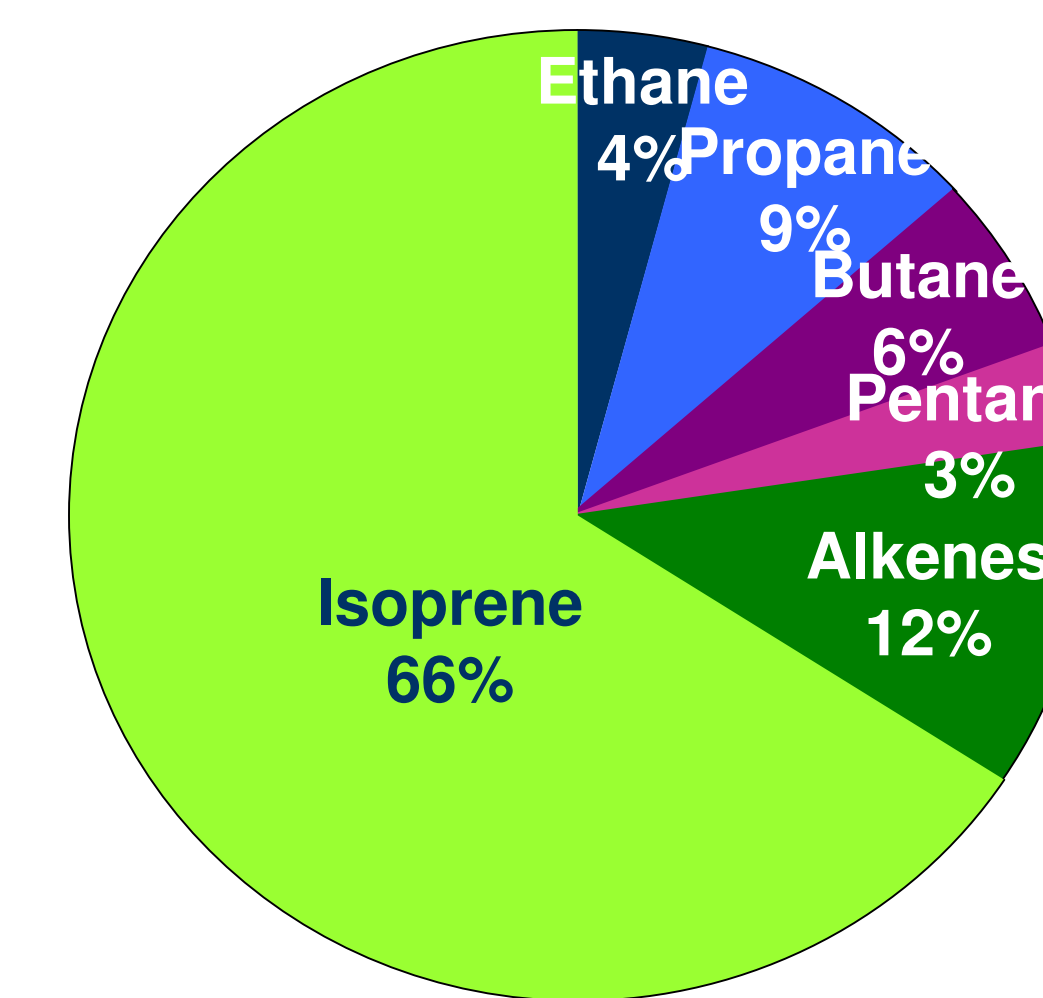


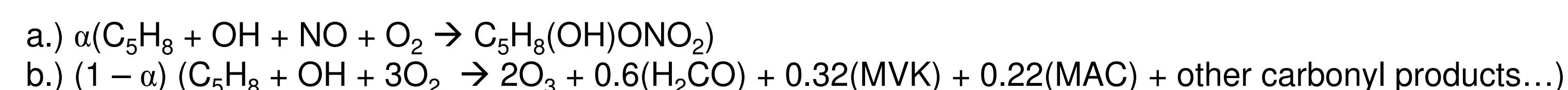
Figure 5: OH reactivity-weighted hydrocarbon budget from third low-level leg of flight on 7/20/2004 (same as Fig. 6). Indicates proportion of  $\text{RO}_2$  that will result from a specified hydrocarbon (assuming the observed molecules represent a complete set). Hydrocarbon data provided by Blake et al, UC Irvine.

By taking both the concentration of isoprene and its OH reactivity into account, it is possible to calculate the proportion of  $\text{RO}_2$  that is isoprene derived. In some locations, as shown in Fig 5, observed isoprene concentrations imply that the majority of available  $\text{RO}_2$  is isoprene-derived. Thus, isoprene nitrates will be a major component of  $\Sigma$ ANs and of  $\text{NO}_y$ . Also, the high solubility of hydroxy-alkyl nitrates produced from isoprene makes them good candidates for both wet and dry deposition to the surface and onto aerosols.

As an illustration of the importance of an accurate branching ratio for isoprene consider the following: if the lowest published nitrate yield of 4.4% is used in conjunction with EPA emission estimates, calculations indicate that up to 7% of NO emissions in the eastern US during the summer are removed through formation of hydroxy nitrates. If, on the other hand, the highest published yield (15%) is used, roughly 20% of the NO emitted is removed through this mechanism. (Chen et al, 1998, Sprengnether, et al., 2002).

## Theoretical correlations between $\text{O}_3$ , $\text{H}_2\text{CO}$ and $\Sigma$ ANs

Isoprene oxidation yields for major products ( $\text{O}_3$ ,  $\text{H}_2\text{CO}$ , MVK and MAC) are fairly well known (Sprengnether, et al., 2002) and the overall oxidation reaction for isoprene can be written as follows:



Where  $\alpha$  is the branching ratio as introduced above ( $k_a/(k_a+k_b)$ ). This overall equation implies the following relationships for an air mass where isoprene is the only important VOC:

$$\frac{\Delta\text{O}_3}{\Sigma\text{ANs}} = \frac{\gamma(1-\alpha)}{\alpha} \sim \frac{2}{\alpha} \quad \frac{\Delta\text{O}_3}{\Delta\text{H}_2\text{CO}} = \frac{\gamma(1-\alpha)}{\beta} \sim \frac{2}{0.6} \quad \frac{\Sigma\text{ANs}}{\Delta\text{H}_2\text{CO}} = \frac{\alpha}{\beta} = \frac{\alpha}{0.6}$$

## Use of field data to constrain nitrate yields

Figures 6 and 7 show correlations between  $\Sigma$ ANs and  $\text{H}_2\text{CO}$  (corrected for photolytic loss of  $\text{H}_2\text{CO}$ ) and  $\Sigma$ ANs and  $\text{O}_3$  respectively with the best fit linear regression, confidence intervals and expected lines for extrema of published branching ratio values. The branching ratios calculated from each individual correlation agree with each other quite well and fall within the range of published values. The correlation between  $\text{H}_2\text{CO}$  and  $\text{O}_3$  (not shown) has a slope of 3.4 which falls within 10% of the 3.17 slope that we would expect to see based on the relative yields. The following plots contain all points below 1 km with the exception of flight 16 on August 6<sup>th</sup>. Correlations made from flight 16 data were considerably different from all of the other flights but the reason for this anomaly is currently unknown.

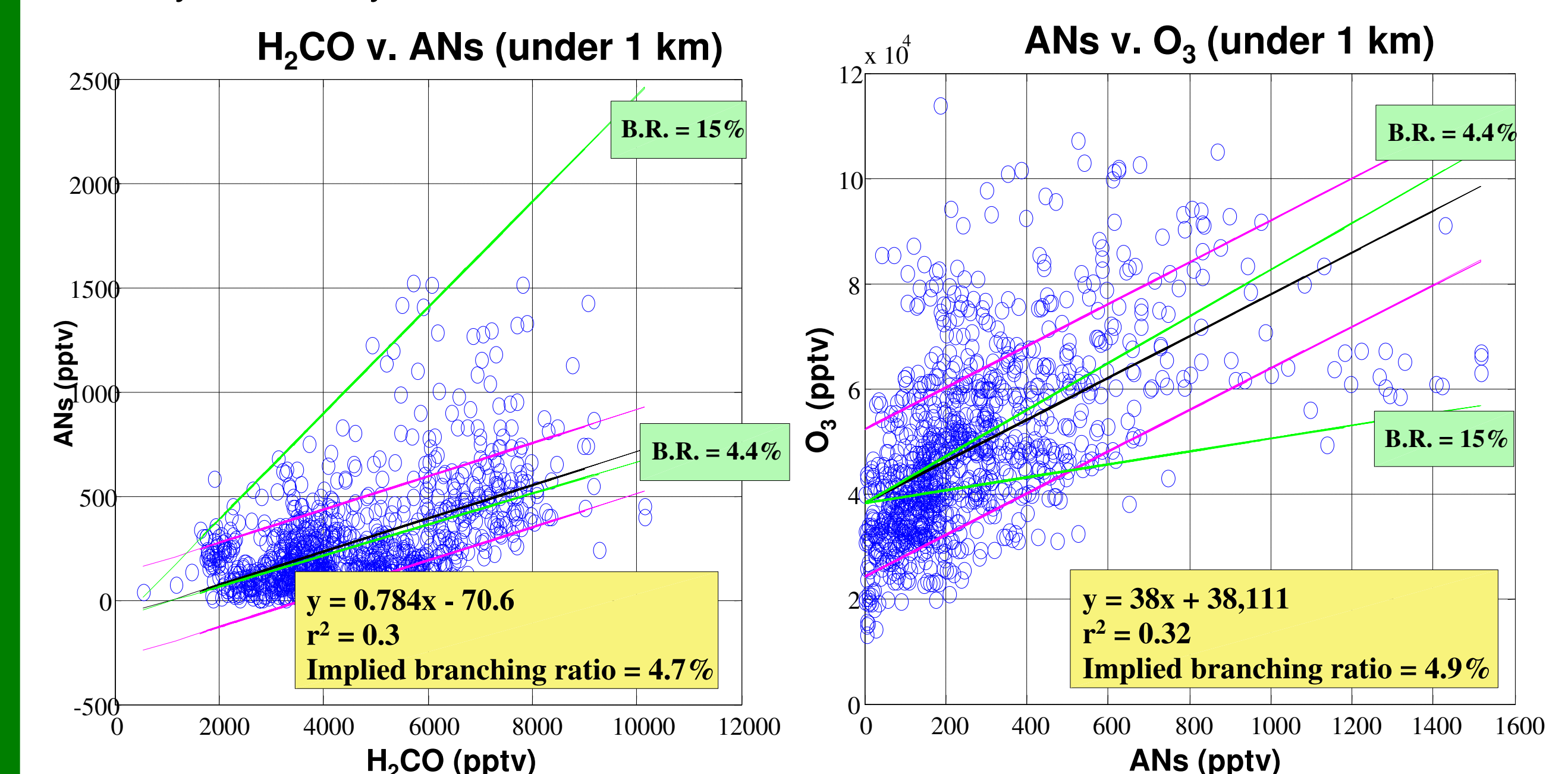


Figure 6:  $\text{H}_2\text{CO}$  v.  $\Sigma$ ANs below 1km. Black line is best fit, pink lines show std deviation. Green lines show what the correlation should look like for maximum and minimum published branching ratio values.

Figure 7:  $\Sigma$ ANs v.  $\text{O}_3$  below 1km. Black, pink and green lines defined as in Fig. 6.

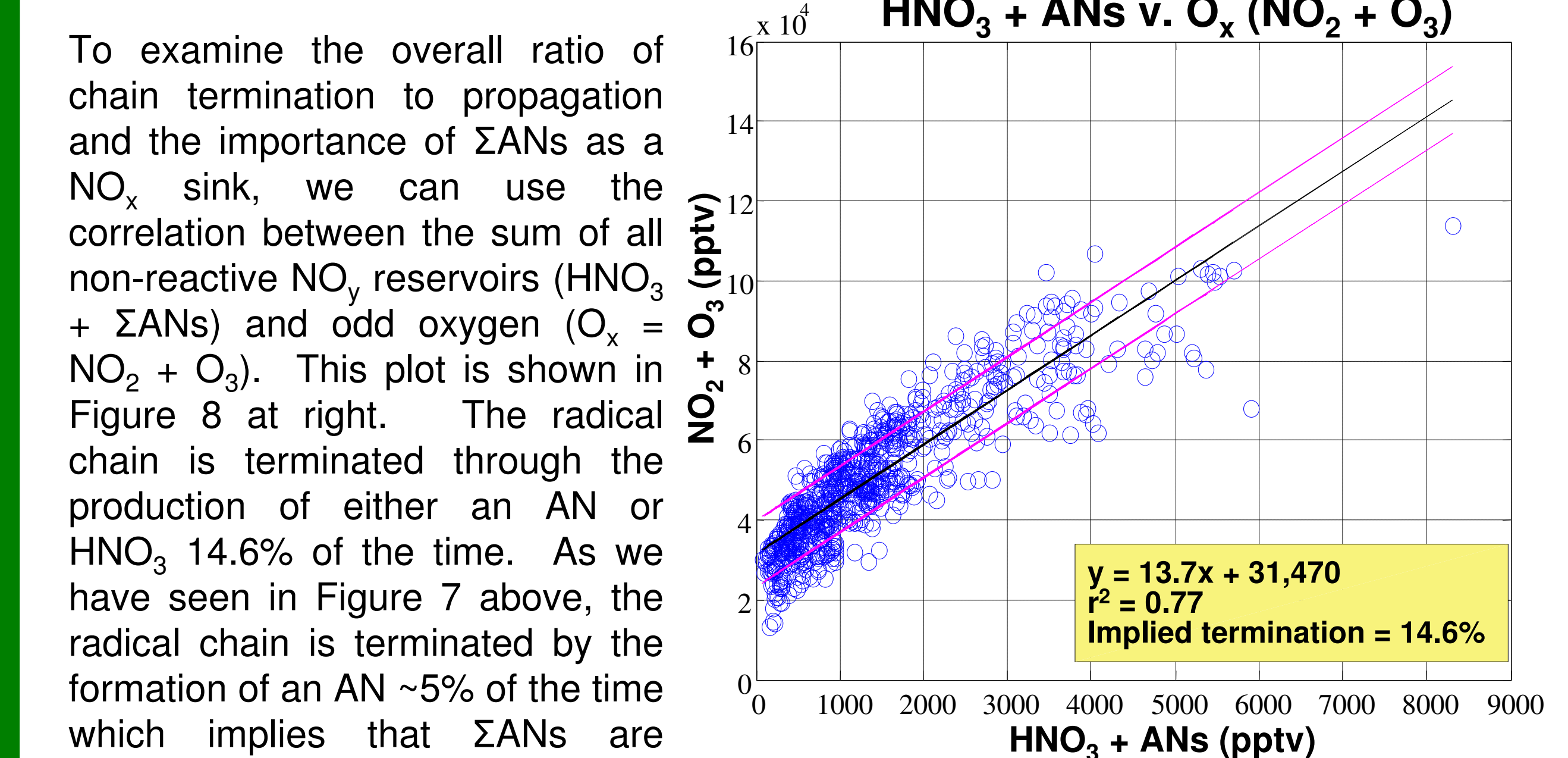


Figure 8: Non reactive  $\text{NO}_y$  ( $\text{HNO}_3 + \Sigma\text{ANs}$ ) v.  $\text{O}_x$  ( $\text{NO}_2 + \text{O}_3$ ) below 1km with best fit line (black) and standard deviation (pink).

## Acknowledgements

- Formaldehyde data provided by Fried et al., NCAR.
- Hydrocarbon data provided by Blake, et al. UC Irvine
- Nitric acid data courtesy of Dibb, et al. UNH.
- Ozone data courtesy of Avery et al.

## References

1. Arey et al, *J. Phys. Chem. A*, Vol. 105, No. 6, 1020, 2001.
2. Chen et al, *J. Geophys. Res.*, Vol. 103 (D19), 25,563, 1998.
3. Chuong and Stephens, *J. Geophys. Res.*, Vol. 107 (D13), 4162, 2002.
4. Day et al, *J. Geophys. Res.*, Vol. 108 (D16), 4501, 2003.
5. Guenther et al, *J. Geophys. Res.*, Vol. 100, 8873, 1995.
6. O'Brien et al, *J. Phys. Chem. A*, Vol. 102, No. 45, 8903, 1998.
7. Sprengnether et al, *J. Geophys. Res.*, Vol. 107 (D15), 4268, 2002.
8. Tuazon and Atkinson, *Int J. Chem. Kin.*, Vol. 22, 1221, 1990.